Contribution to Radio Frequency Generation in Regards to MCG

M. M. Kekez
High-Energy Frequency Tesla Inc. (HEFTI)
1200 Montreal Road, Bldg. M-51, Ottawa, ON, Canada, K1A 0R6
E-mail: mkekez@magma.ca

***Abstract*— The spectral power density versus frequency of the electrically-driven RF system are compared with the data of MCG by Prishchepenko *et al.* [1]. It is suggested that they have the common mechanism of RF generation at low frequency range.**

I. Introduction

The use of a small MCG to produce compact radio frequency (RF) sources was disclosed by A. B. Prishchepenko in a paper delivered at the EUROEM Conference in Bordeaux, France, 1994. In this paper, Prishchepenko *et al.* [2] [1] described how these RF sources might be used for military purposes. This reported development of RF sources raised concern in many countries. Merritt [3] presented an assessment of the significance of these developments to the Joint Economic Committee of the US Congress 1998. Kopp [4] has published papers of the design of RF weapons and their potential effects.

To understand the mechanism of RF generation, it is useful to consider this as a two-step process. The first step is the conversion of the chemical energy stored in the explosive into electrical energy. The second step is the conversion of the electrical energy into electromagnetic energy of radiation.

The second step can be simulated by the electrostatic energy deposited in the capacitor (Marx) bank and/or by the magnetic energy stored in the coil. With this approach, the laboratory equipment is not destroyed with each test. Several electrically-driven RF systems have been developed to help us understand the mechanism of RF generation and to have an assessment of the RF vulnerability of computer and digital systems against these RF radiations.

In open literature there are few information about the value of RF fields. For example, Kekez [5] has demonstrated that the electrically-driven RF system can produce the RF power of above one gigawatt. The energy stored in the Marx bank was equivalent to a few milligrams of explosive. The generation of RF emissions above 100 MHz was also demonstrated by Kekez [6]. Altgilbers *et al.* [7] have proposed that the emission could be the result of nonlinear coupling of inductive and capacitive loads in MCGs. Their computer simulations spectrum resides in the 0.1 to 1.0 GHz frequency band. Altgilbers *et al.* [8] have demonstrated that a single gas-filled spark gap placed in H-waveguides is capable of producing broadband pulse in the frequency range of 0.4 to 0.8 GHz. A useful interpretation of the mechanism of RF generation from MCGs has been put forward by Tracy *et al.* [9]. In this report the experimental data obtained with the electrically driven RF source are compared with the data of Prishchepenko *et al.* [1]

II. Results

A 10-stage mini-Marx of the design similar to that given in [10] was used to energize the RF source. The spectrum of the emission was observed to be broad ranging from tens of MHz to over 20 GHz and containing a large number of distinctive lines. From 20 MHz to about 2 GHz, the detailed measurements were carried out using the 10 GHz D-dot probe made by Prodyne Inc. The strength of the electrical field, E was calculated according to the formula given in [6] and the power density, p is defined as $E^2/(2Z_0)$ where $Z_0 = 377\ \Omega$. The maximum value of the measured electric field is given in Table I at several frequencies.

To make the analysis possible of the experimental data, the method was found to "tune" the RF source to radiate mainly at the single frequency. The idea is being submitted for the patents applications. The theoretical model has been derived to evaluate the current and voltage waveforms, as well as the available energy deposited in RF source. The results are shown in Figure 1. The voltage is modulated and the current trace is a semi-smooth function of time. These modulations are causing the radio frequency emissions. In the theoretical model, the Marx generator was presented as the capacitor of 1 nF charged at 100 kV with the closing switch. The internal impedance of the Marx generator is 10 Ω. If the RF source is replaced by the resistive load, the Marx generator would produce a double-exponential pulse of a short rise-time and long exponential fall.

If the relative dielectric constant, ϵ_r of all the insulating material used is one, the main frequency of the modulation is:

$$f = \frac{c}{4l} \tag{1}$$

c is the velocity of light and l is the longitudinal length of RF source. Equation 1 can be confirmed if the length of the leads, L connecting RF source to the Marx generator are short in comparison to l, i.e. $l \gg L$.

To minimize the corona discharges taking place at the head of RF source, the head must be shaped in the form of hemisphere. This arrangement provides an additional capacitance, C formed between the head and the ground. For $l = 30$ cm and $\epsilon_r \approx 1$, according to Equation 1, $f = 250$ MHz. Because of C (=0.8 pF), the frequency, f is lowered to 217 MHz. See Figure 1. The frequency of 657 MHz shown in FFT

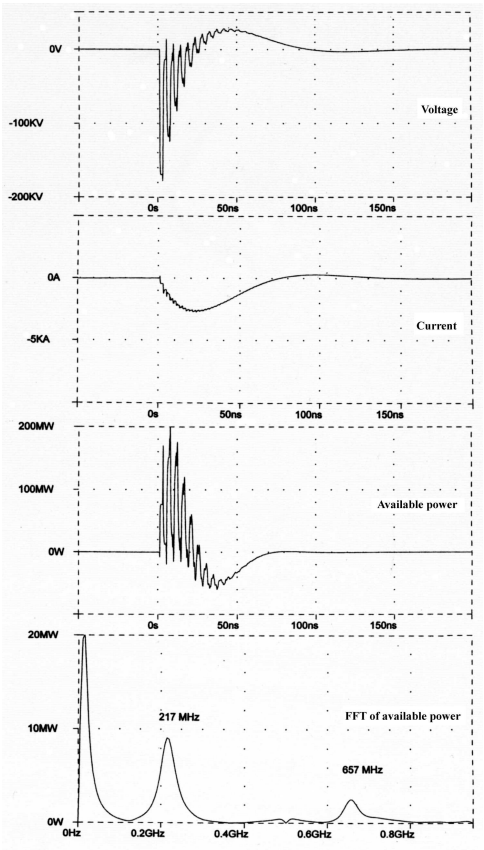

Fig. 1. Computer simulation of voltage, current and the available power supplied to the RF device.

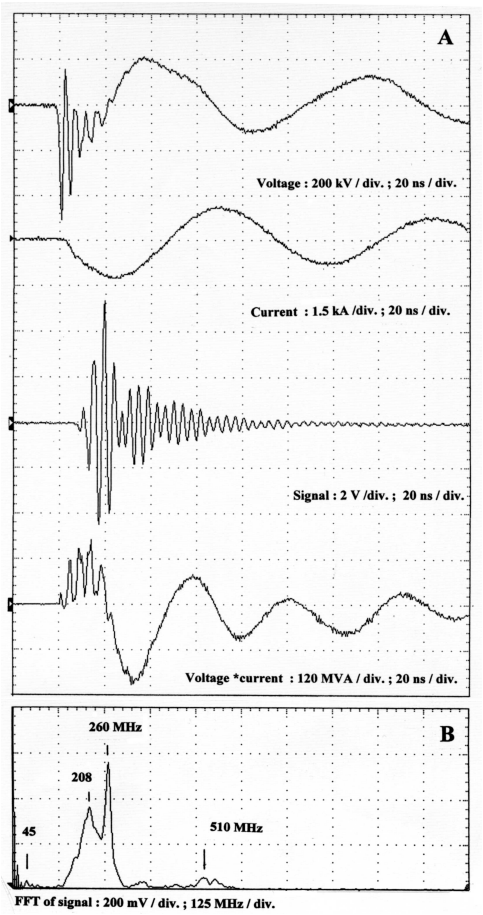

Fig. 2. Experimental data of voltage, current and the available power supplied to the RF device at charging voltage of 35 kV/stage. 550 MHz low-pass filter was used in order to get a "clean" signal waveform.

corresponds to the harmonic of f=217 MHz. The available power is the product of voltage times current and is measured in volts$\times$amperes and it is not in watts as indicated in Figure 1.

Figure 2 offers the experimental verification of the theoretical model indicated in Figure 1. To obtain the scaling laws, the RF energy contained in the pulse was measured as a function of the charging voltage applied to the Marx generator. The results are given in Figure 3. The experimental point marked by square is the average value of five measurements. The solid line is the regression curve. The RF energy was obtained by multiplying the RF signal by itself and by calculating the area under this resulting waveform. The same procedure was used to get Figures 5, 8 and 10.

In Figure 4, Frame B the emissions are at the frequency of 540 MHz with the bands at 1.07 GHz and 2.58 GHz. Figure 4, Frame A and Figure 5 were obtained with a low pass filter of 0.550 GHz. In Figure 4 the trace power means multiplying the signal by itself. When the charging voltage varies from 18 to 23 kV/stage, the frequency band at 1.07 MHz converges towards the single frequency of 1.12 GHz. This is shown in Figure 6.

When the RF source is of longer longitudinal length, Figures 7 and 8 were obtained. By capacitively loading the structure used in Figure 7, Figures 9 and 10 were obtained.

The power density was computed over the solid angle of 4π. The total power was obtained by integrating the power density over the same angle. The resulting graph is the spatial distribution that has the maximums and minimums with its standing wave loops and nodes. The spatial distribution was derived for the frequency of 540, 260, 165, and 137 MHz. Because of the finite size of the anechoic chamber: 20'$\times$12'$\times$10', the field distribution (hence the RF power) was only estimated at f=36 MHz for the conditions of Figure 9.

For frequencies of 36, 165 and 260 MHz, the D-dot probe was placed 1.68 m away from the source, whereas the distance is 1.10 m for frequencies of 550 and 1120 MHz. For the latter data the electrical fields was recalculated for the distance of 1.68 m and the value are presented in Table I. The charging voltage was at 35 kV per stage for all the data given in Table I.

For frequencies above 2 GHz, a suitable combination of horns, bandpass filter and crystal diodes were used. Particular attention was given to the domain from 8.2 to 12.4 GHz and 12.4 to 18 GHz. The results are given in Figure 11. The work shows that the origin of these emissions are due to the spark discharges. All the attempts to organize these discharges to yield a significant amplification of HPM signal at particular frequency have not been so far successful. Their spectral power

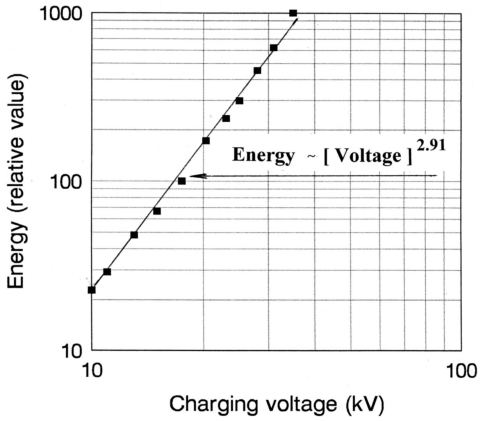

Fig. 3. RF energy of pulse, E vs. charging voltage, V. Scaling law is $E \sim V^{2.91}$ at 260 MHz.

TABLE I

ANALYSIS OF THE EXPERIMENTAL DATA

Frequency, f (MHz)	36	165	260	540	1120
D-dot max. amplitude, V, (V)	6.4	8.3	8.6	6.2	2.15
Electric field, E (kV/m)	320	90	60	20	3.4
Power density, p (MW/m^2)	135	10.8	4.7	0.53	0.016
Power, P (MW)	600	48	21	0.58	0.0173
Spectral power density, S (W/Hz), where $S = P/f$	16.8	0.29	0.081	0.001	1.5×10^{-5}
See Figure	9	7	2	-	-

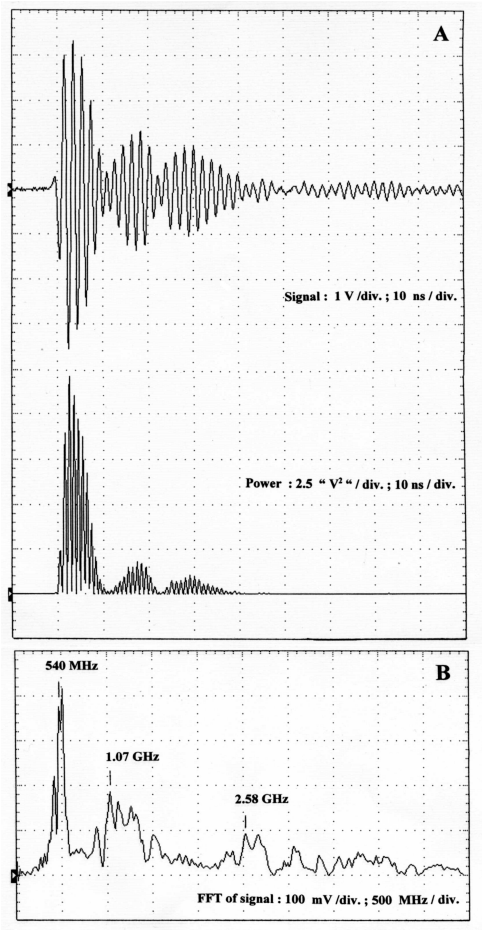

Fig. 4. Emissions at 540 MHz. Charging voltage is 26 kV/stage. Probe is at 110 cm away from the source. Frame A: Signal and power with 550 MHz low-pass filter placed between the probe and the oscilloscope. Frame B: FFT of unfiltered RF emissions.

density recorded was well below 10^{-5} W/Hz. The power value of Figure 11 means the voltage reading as it was recorded on the oscilloscope.

III. DISCUSSION

At the main frequency of oscillation at 217 MHz of Figure 1, the RF energy in the pulse, E scales as $E \sim V^2$ where V is the charging voltage per stage of the Marx generator. The theoretical model suggests that the fixed proportion of the energy stored in the Mini-Marx generator in form of $CV^2/2$ is converted into RF emissions. From Figures 3, 5, 8 and 10, we see that the exponent is larger than 2. This occurs because at higher charging voltage, the system can be better "tuned" to the single frequency. We see from FFT that the amplitudes of harmonics and other frequency bands in regards to the main frequency are decreased as the charging voltage rises. Also at higher voltage, the internal impedance of the Marx generator is decreased, which in turn yields to higher efficiency of RF generation as it is confirmed by the theoretical calculations.

IV. CONCLUSION

The theoretical model of the RF generation confirms the experimental findings in the range from 30 MHz to about 1 GHz. It was observed that the amplitude of the D-dot RF signal is of the same order for the frequencies from 20 to 540 MHz. Also for the same frequency range, the equivalent area by which the power density is multiplied to get the power is again of the same order of magnitude.

The spectral power density (W/Hz) versus frequency (f) of Table I is given in Figure 12, which suggests that the electrically-driven RF system and MCG may have the common mechanism of RF generation at low frequency range.

REFERENCES

[1] Prishchepenko A. B. and Shchelkachev M. V., 1996, "The work of the explosive type generator with capacitive load," *Proceedings of Megagauss VII Magnetic Field Generation and Pulsed Power Applications*, Sarov, Russia, pp 304-307

[2] Prishchepenko A. B. and Shchelkachev M. V., 1993, "Dissipation and Diffusion losses in a spiral explosive magnetic generator," Electrichesvo, N. 8. pp 31-36

[3] Merritt I. W., 1998, "Proliferation and Significance of Radio Weapons Technology before the Joint Economic Committee" http://www.house.gov/jec/hearings/radio/merritt.htm

[4] Kopp C., "The e-bomb-a weapon of electrical mass destruction, Department of Computer Sciences," Clayton, Australia, http://www.inforwar.com/mil_c4i/mil_c4i8.html-ssi

[5] Kekez M. M., 2001, "A compact square waveform 15 kJ generator: ¡15 ns rise-time; 7.5S load impedance and pulse width: 100-500 ns," *13th IEEE Conference on Pulsed Power-Plasma Science*, Las Vegas, Nevada, USA, 17-23 June, pp 1027-1030

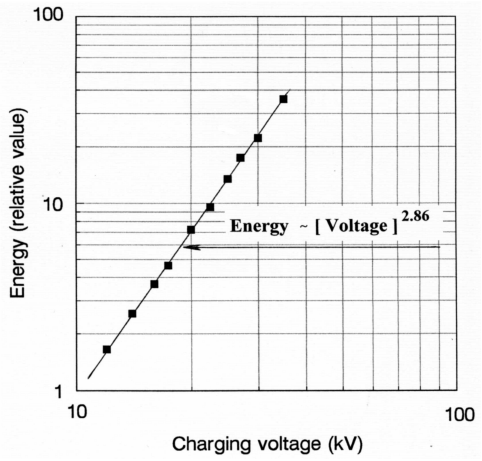

Fig. 5. RF Energy of pulse, E vs. charging voltage, V. Scaling law is $E \sim V^{2.86}$ at 540 MHz.

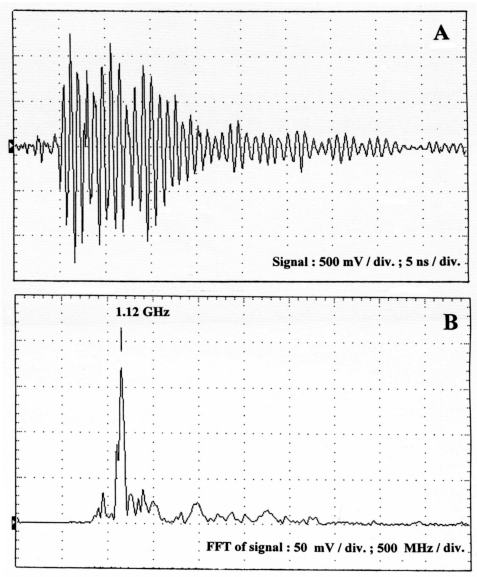

Fig. 6. Emissions at 1.12 GHz. Charging voltage is 26 kV/stage. Other condition as in Figure 4, except that 1 GHz high-pass filter was used.

[6] Kekez M. M., 2003, "High repetition rate compact Marx generator," *IEEE Conference on Pulsed Power,* Dallas, Texas, USA, 15-18 June, 2003, pp 1427-1430

[7] Altgilbers L. L., Tkach Yu V., Yatsenko T. and Tkach Ya, 2003, "Non-linear reactive circuits driven by magnetic flux compression generators," *14th IEEE Int. Pulsed Power Conference,* Dallas, Texas, USA, pp 1085-1088

[8] Altgilbers L. L., Somov V. A., Chepurniy Ia, Tkach Yu V. and Silin A. O., 2003, "Broadband pulsed generator based on H-waveguides," *14th IEEE Int. Pulsed Power Conference,* Dallas, Texas, USA, pp 1073-1077

[9] Tracy P., Altgilbers L. L., Brown M. and Merritt I., 1996, "Inductive Electromagnetic Field Generators," *Proceedings of Megagauss VII Magnetic Field Generation and Pulsed Power Applications,* Sarov, Russia, pp 308-313

[10] Kekez, M.M, 1991, "Simple sub-50-ps rise-time high voltage generator," *Rev. Sci. Instrum.* 62, pp 2923-2930

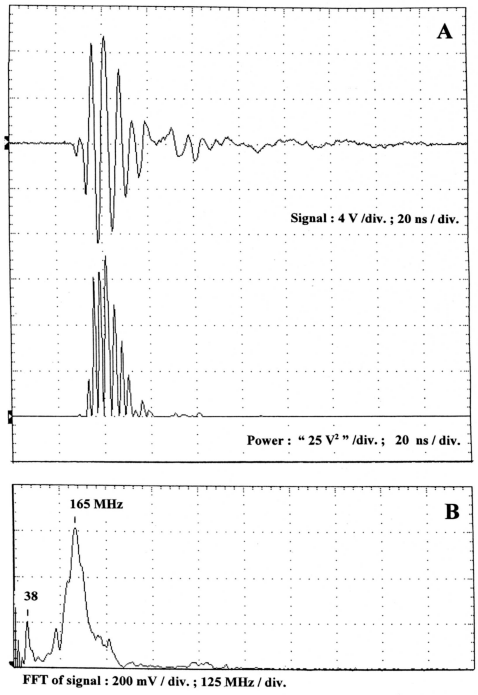

Fig. 7. Emissions at 165 MHz. Charging voltage is 35 kV/stage. Probe is at 1.68 m away from the source. A low pass filter of 0.550 GHz was applied.

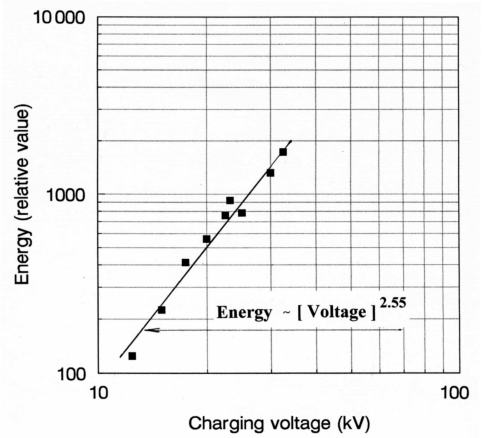

Fig. 8. RF energy of pulse, E vs. charging voltage V. Scaling law is $E \sim V^{2.55}$ at 165 MHz.

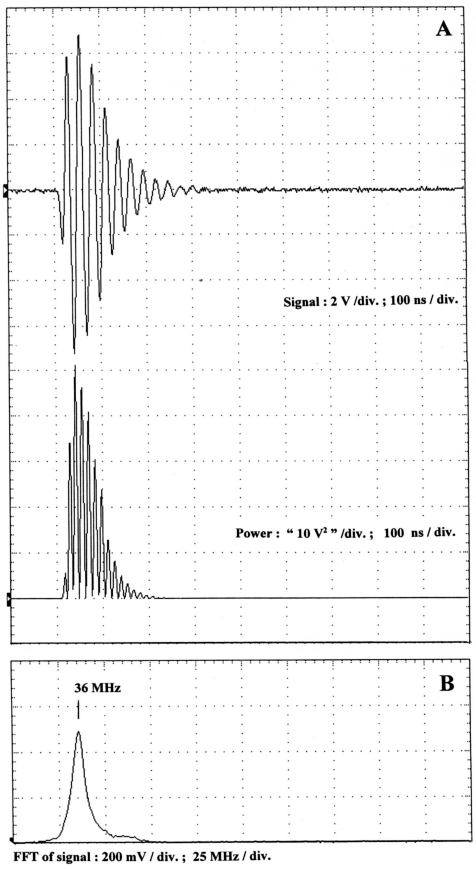

Fig. 9. Emissions at 36 MHz. Charging voltage is 35 kV per stage. Probe is at 168 cm away from the source.

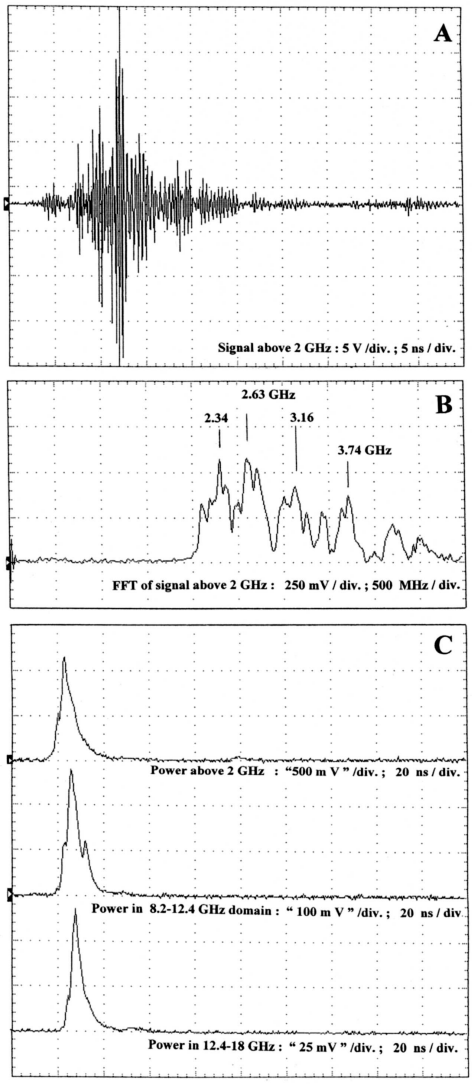

Fig. 11. Emissions recorded with horns and crystal detector. Charging voltage is 26 kV/stage. All horns are placed 2 m away from the source. Signal obtained with 2 GHz horn is shown in Frame A and its FFT is given in Frame B. Power recorded for different frequency range is shown in Frame C. The amplitude of power is the voltage reading at the oscilloscope.

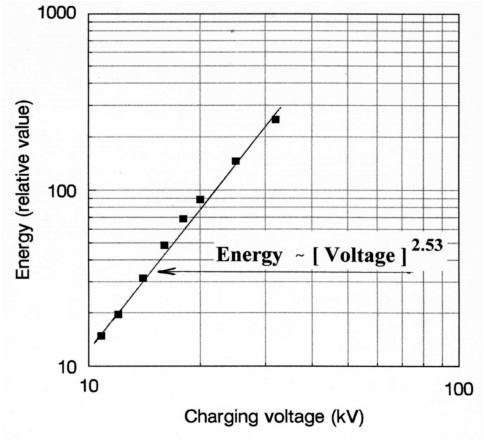

Fig. 10. RF energy of pulse, E vs. charging voltage, V. Scaling law: $E \sim V^{2.53}$ at 36 MHz.

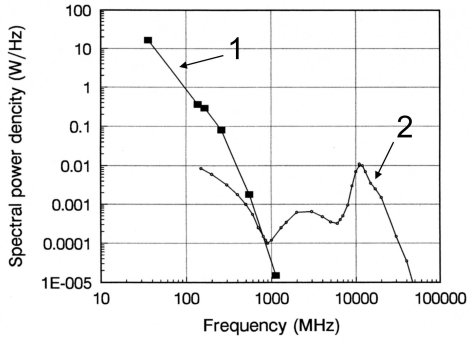

Fig. 12. Spectral power density (watts/f) vs. frequency (f). The curve #1 is the current measurements. The curve #2 is after Prishchepenko *et al.* [1].